Evolution of magnetic structures in $NpAs_{1-x}Se_x$ solid solutions

A. Bombardi
Département de la Recherche Fondamentale sur la Matière Condensée, Commissariat à l'Energie Atomique-Grenoble, F-38054 Grenoble, France
and European Commission, Joint Research Centre, Institute for Transuranium Elements, Postfach 2340, D-76125 Karlsruhe, Germany

F. Bourdarot, P. Burlet, J. P. Sanchez, and P. Vulliet
Département de la Recherche Fondamentale sur la Matière Condensée, Commissariat à l'Energie Atomique-Grenoble, F-38054 Grenoble, France

E. Colineau, J. Rebizant, F. Wastin, and G. H. Lander
European Commission, Joint Research Centre, Institute for Transuranium Elements, Postfach 2340, D-76125 Karlsruhe, Germany

O. Vogt and K. Mattenberger
Laboratorium für Festkörperphysik, ETH-Zürich, CH-8093 Zürich, Switzerland
(Received 27 July 2000)

We report Mössbauer spectroscopy, magnetization, and neutron-diffraction measurements on four samples ($x=0.05$, 0.10, 0.15, and 0.20) in the mixed system $NpAs_{1-x}Se_x$. The evolution of magnetic phase diagram vs the temperature T and the Se concentration x has been determined. Up to $x=0.15$, three distinct phase transitions are present. The first antiferromagnetic (AF) at $T_N(x)$ is from paramagnetism to an incommensurate phase, the second, at $T_C(x)$, is to a ferromagnetic (FM) phase, the third at $T_m(x)$ is from pure FM to a mixed phase where AF and FM ordering coexist along perpendicular directions. The temperatures of the transitions are functions of Se concentration x. The incommensurate structure is described by a longitudinal amplitude modulated sinusoidal wave with a wave vector $\vec{k}$ in the range (0 0 0.14–0.24) that is shifted toward the center of the Brillouin zone with increasing x. A squaring up of this wave, if present, is too small to be detected. At $T_C(x)$ all Np sites become equivalent and the moment directions become $\langle 1\,1\,1\rangle$. Surprisingly, at $T_m(x)$ AF interactions again become important and cause the moments to rotate and to align along $\langle 221\rangle$ directions. Measurements in an external magnetic field up to 4.8 T have allowed us to determine the $1\vec{k}$ nature of the AF component for $T<T_m$ and to establish the moment directions. Increasing Se content reduces the incommensurate phase to a small range of T and reduces the AF interactions. At $x=0.20$ pure FM behavior, as shown by the magnetization measurements, is recovered. The saturated Np moments at low T decrease slightly with increasing x.

I. INTRODUCTION

The solid solutions that we have studied are made by a combination of a Np monopnictide with a Np monochalcogenide. The parent compounds belong respectively to the light actinide (An=U, Np, Pu) monopnictides AnX (X=N, P, As, Sb, Bi) and monochalcogenides AnY (Y=S, Se, Te) families, all with the fcc NaCl-type structure. Since the beginning of research on transuranic compounds, these families of compounds have been studied widely. But, despite considerable experimental[1] and theoretical efforts,[2] their physical behavior is far from understood. With respect to magnetism, the UX compounds are all antiferromagnets (AF) and the UY are all ferromagnets (FM), but this simple division is not found in the analogous Np compounds, and possibly the biggest surprise is the lack of any magnetism in the PuY compounds.[3,4] In Table I we report the known magnetic properties of NpX and NpY compounds. The lattice parameters (a) are large enough to prevent direct overlap between $5f$ electrons, so hybridization and exchange play a crucial role, and must involve both the conduction electrons and the anion p states. With the exception of NpN, which is ferromagnetic, the NpX materials show AF order with components along $\langle 001\rangle$, and an interplay of $1\vec{k}$ and $3\vec{k}$ structures that is found in abundance in the UX compounds.[5,6] The behavior of the NpY compounds is substantially different from that of the NpX systems. Although they all show AF order, the ordering is of type II, which consists of alternating (111) FM planes rather than the (001) planes in the type-I arrangement, and there are drastic reductions in the ordering T_N (by about a factor of 5) and in the magnetic moment values. Moreover, the paramagnetic Curie temperatures (θ_p) are negative whereas they are positive in the NpX compounds. The exact moment directions in the NpY compounds are not yet completely solved as a number of possible multi-$\vec{k}$ configurations are possible.[5]

The present experiments start with NpAs and proceed to add Se. Substituting Se adds one p electron, presumably to the conduction band, thus modifying the chemical potential and the hybridization. Studies of this sort have been pursued mainly in the UX-UY systems,[5,6] whereas in the Np-based systems only studies in the NpSb-NpTe system are available.[7] Despite both the parent compounds being AF,

TABLE I. Lattice parameter a and some magnetic properties of NpX and NpY compounds. $T_{N,C}$ indicates a transition from paramagnet to an ordered magnetic structure, T' indicates a transition between different magnetic structures. $\vec{k}$ is the propagation vector of the observed magnetic structures. m_0 is the ordered magnetic moment measured by neutron diffraction at low temperatures (LT) and μ_{eff} is the paramagnetic moment.

	a (Å)	$T_{N,C}$ (K) T' (K)	θ_p (K)	$\vec{k}$	Easy axis	Magnetic ordering	m_0 (LT) (μ_B)	μ_{eff} (μ_B)
NpN	4.897	87	86	$\langle 0\,0\,0\rangle$	$\langle 1\,1\,1\rangle$	FM	1.4	2.13
NpP	5.615	120	96	$\langle 0\,0\,1/3+\varepsilon\rangle$		$2\vec{k}$, Inc.		
		95	70	$\langle 0\,0\,1/3+\varepsilon\rangle$		$3\vec{k}$, Inc.		
		70		$\langle 0\,0\,1/3\rangle$	$\langle 0\,0\,1\rangle$	$1\vec{k}\,3+3-$	1.9	2.85
NpAs	5.838	173	184	$\langle 0\,0\,0.233\rangle$	$\langle 0\,0\,1\rangle$	$1\vec{k}$ Inc.		
		154		$\langle 0\,0\,1/4\rangle$	$\langle 0\,0\,1\rangle$	$4+4-1\vec{k}$		
		138		$\langle 0\,0\,1\rangle$	$\langle 1\,1\,1\rangle$	$3\vec{k}$ type I	2.6	2.82
NpSb	6.254	200	150	$\langle 0\,0\,1\rangle$	$\langle 1\,1\,1\rangle$	$3\vec{k}$ type I	2.5	2.56
NpBi	6.438	192.5	114	$\langle 0\,0\,1\rangle$	$\langle 1\,1\,1\rangle$	$3\vec{k}$ type I	2.63	2.90
NpS	5.527	$\simeq 22$	-81	$\langle 1/2\,1/2\,1/2\rangle$	?	? type II	0.8	2.1
NpSe	5.804	38	-130	$\langle 1/2\,1/2\,1/2\rangle$	?	? type II	1.1	1.9
NpTe	6.198	42	-105	$\langle 1/2\,1/2\,1/2\rangle$	?	? type II	1.4	2.3

5% doping of Te is enough to induce a mixed magnetic ordering at low T, resulting from a FM component along $\langle 1\,1\,0\rangle$ and an AF one along $\langle 0\,0\,1\rangle$. The authors concluded that moments are alternatively close to $\langle 111\rangle$ and $\langle 11\overline{1}\rangle$. At 10% doping of Te the solid solution is purely FM with moments along $\langle 1\,1\,1\rangle$.

Pure NpAs and NpSe compounds have been studied by various techniques. NpAs orders at $T_N \simeq 173$ K (Refs. 8 and 9) into an incommensurate $1\vec{k}$ state, has a lock in transition to a commensurate $(4+,4-)$ phase at $T_{IC} \simeq 154$ K,[10,11] and then again at $T_o = 138$ K a first-order transition occurs to a $3\vec{k}$ state of type I. This latter transition forces the lattice symmetry to be cubic, so the small tetragonal distortion observed when the AF order is $1\vec{k}$ is removed.[11] The low-temperature magnetic moment is about $2.5\mu_B$ close to the free Np^{3+} ion value in intermediate coupling ($2.57\mu_B$). At 4.2 K, an external magnetic field induces a FM component resulting in a mixed AF-FM phase ($\vec{H}$ between 4 and 6 T). The easy axis is $\langle 1\,0\,0\rangle$, up to 10 T the system stays in this mixed phase.[9] Resistivity measurements[12] show the traces of the phase transitions, at low T NpAs is a semimetal. Mössbauer measurements at 4.2 K are well fitted with a single Np^{3+} site and the hyperfine field corresponds to a magnetic moment of $2.52\mu_B$.[13]

The situation for NpSe is less clear. It displays a second-order transition to an AF type-II phase ($\vec{k}=[\frac{1}{2}\,\frac{1}{2}\,\frac{1}{2}]$) at 38 K with $\vec{m}_{\vec{k}} \perp \vec{k}$ but the actual structure has not been determined. The two more realistic possibilities seem to be a $2\vec{k}$ or a $3\vec{k}$ structure with possibly two different magnetic Np sites. The magnetic moment is about $1.2\mu_B$, much lower than the free-ion value. Mössbauer spectra[14] at low T present broad line shapes. This, together with the higher average magnetic moment ($1.4\mu_B$) estimated from the Mössbauer data, suggest that long-range ordering coexists with short-range magnetic correlations.

In the present paper we report ^{237}Np Mössbauer spectroscopy, magnetization, and neutron-diffraction measurements. Mössbauer spectroscopy is a local probe that gives the hyperfine Hamiltonian parameters, allows the determination of the valence state of the Np ions, and of the magnetic moment value at the Np sites. Magnetization and neutron-diffraction on single crystals gives information on the easy direction of magnetization and details of the magnetic structures, respectively, as well as the value of the moments.

II. EXPERIMENT

Crystals were grown by mineralization technique.[15] For each given x, all samples came from the same batch. The growth process gives a confidence level on nominal stoichiometry of about 1%.

Mössbauer measurements were performed on crushed single crystals at 4.2 K. The source was a foil of ^{241}Am metal. The Mössbauer velocity scale was calibrated with reference to a $NpAl_2$ absorber ($B_{hf} \simeq 330$ T at 4.2 K). Hyperfine interaction parameters were obtained by least-square fitting of the absorption spectra using an appropriate effective hyperfine Hamiltonian.

For magnetization measurements crystals were oriented along the main crystallographic axes. Magnetization measurements have been made at ETH Zürich and ITU Karlsruhe using moving sample magnetometers in field up to 10 T and a superconducting quantum interference device up to 7 T, respectively.

Neutron-diffraction measurements have been made using the D15 diffractometer, installed at the ILL high flux reactor, working in the normal-beam geometry. The advantage of this geometry is the possibility of monitoring both the in scattering-plane and the out of scattering-plane reflections (up to 35°). All the samples for the neutron experiments (single crystals of a few mm^3) were oriented with a twofold axis vertical and mounted in a cryomagnet with maximum

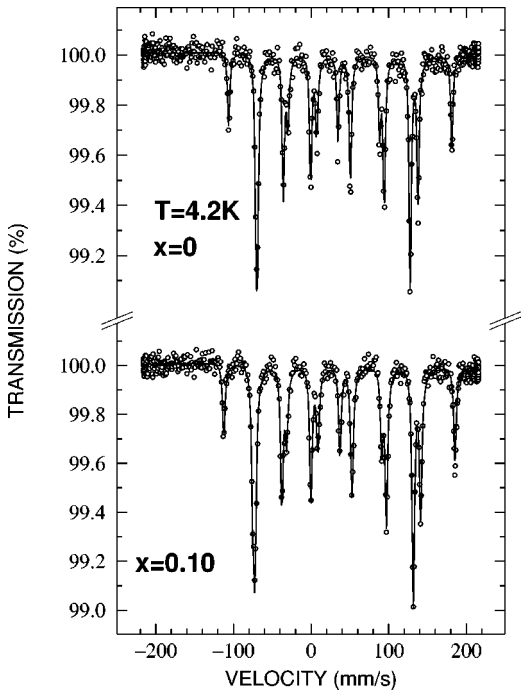

FIG. 1. ^{237}Np Mössbauer spectra for NpAs and $NpAs_{0.90}Se_{0.10}$ at 4.2 K.

obtainable field of $\simeq$4.8 T and temperature control between 5 and 300 K. Data were corrected for absorption. Due to high symmetry of the NaCl crystal structure only two structure factors are present. This prevents a refinement of all structural parameters (scale factor, Debye-Waller factors, extinction correction, and stoichiometry) at the same time. We assumed nominal stoichiometry and reasonable Debye-Waller factors in order to estimate the scale parameter and extinction factor in the paramagnetic phase. The extinction changes between the ferromagnetic and paramagnetic phases but the presence of the FM contribution makes it difficult to estimate the new extinction parameter at low temperature. We have therefore estimated magnetic moments by using only weak reflections at low angles.

III. MÖSSBAUER SPECTROSCOPY

As shown in Fig. 1, the Mössbauer spectra at 4.2 K of pure NpAs and of the diluted samples are very similar. The well resolved magnetic hyperfine splitting unambiguously indicates the presence of magnetic order. The spectra of all the investigated compounds were fitted assuming a single Np site experiencing both electric and magnetic hyperfine interactions. The small hyperfine field and quadrupolar spreads due to local environment effects when $x>0$ manifest themselves as a slight increase of the Lorentzian linewidths W ($W\simeq$3.5 mm/s and 4.9 mm/s for $x=0$ and 0.20, respectively). It is worth mentioning that an induced electric-field gradient is present in the ordered state although the Np ions are in cubic symmetry (at least in the $3\vec{k}$ type-I magnetic structure). The values of the isomer shift δ_{IS} [Fig. 2(c)] allow a Np^{3+} charge state to be assigned for all $NpAs_{1-x}Se_x$ studied compounds. Furthermore, the value of the quadrupole interaction parameter e^2qQ in NpAs (-28.6 mm/s) is very close to the free Np^{3+} ion estimate (-27.3 mm/s), which confirms the occurrence of such a charge state.[16]

Figure 2(a) shows that the hyperfine field (B_{hf}) exhibits a maximum value at $x\simeq$0.05–0.10 whereas $|e^2qQ|$ decreases and δ_{IS} increases continuously when raising the Se content. Notice that B_{hf}, proportional to $\langle J_z\rangle$ in a first approximation, is close to the free ion Np^{3+} value ($\sim$5300 kOe) whereas e^2qQ related to $\langle 3J_z^2-J(J+1)\rangle$ is strongly reduced when x increases. The latter behavior indicates that $\langle J_z^2\rangle\simeq\langle J_z\rangle^2$ and in turn $\langle J_z\rangle$, i.e., the Np magnetic moment decreases monotonously when substituting As with Se. Thus the small increase ($\sim$3%) of B_{hf} observed between $x=0$ and $x=0.05$ is attributed to a change of magnetic structure which induces a different transferred hyperfine field contribution to B_{hf}.[17] These conclusions are nicely corroborated by the neutron-diffraction results discussed in Sec. V.

IV. MAGNETIZATION MEASUREMENTS

At high T all the samples show a Curie-Weiss behavior of the susceptibility with an effective magnetic moment (μ_{eff}) close to the free Np^{3+} ion value and slightly decreasing θ_p with increasing x as shown in Table II. Magnetization curves at high T in small field for $x=0.05$ clearly show two magnetic phases with a first-order transition around 157 K, see Fig. 3. Hysteresis loops at low T have been measured for the

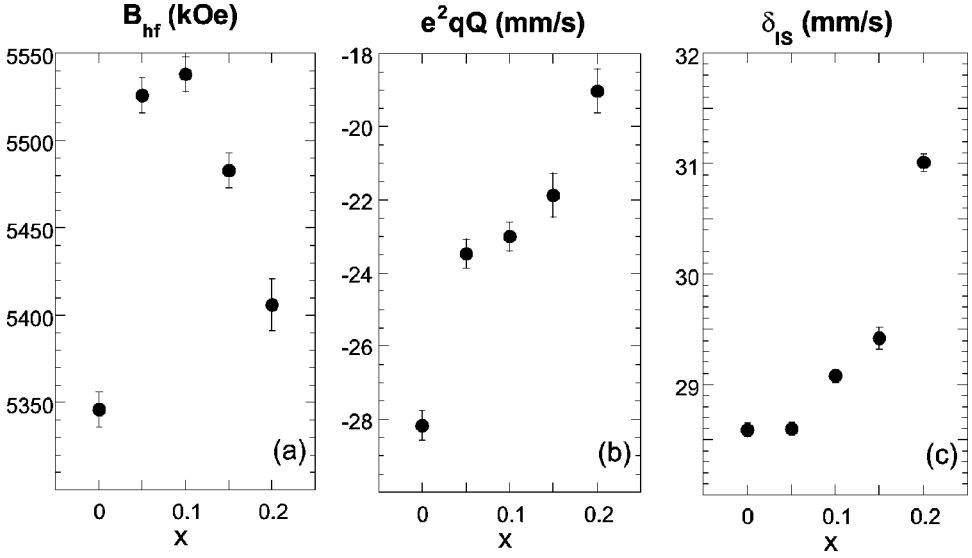

FIG. 2. ^{237}Np hyperfine parameters in $NpAs_{1-x}Se_x$ at 4.2 K. The isomer shift is relative to the ^{241}Am metal source.

TABLE II. Some of the symbols are defined in Table I. The new ones are the FM component (m_{FM}), the AF moment (m_{AF}), and the total moment m, that are measured by neutron diffraction at low T. The saturated moment m^* is obtained by magnetization measurement along $\langle 1\,1\,1\rangle$.

x	a (Å) RT x rays	m_{FM} (μ_B)	m_{AF} (μ_B)	m^* (μ_B)	m (μ_B)	θ_p (K)	μ_{eff} (μ_B)
0	5.8383(3)		2.6(1)		2.6(1)	184	2.82
0.05	5.8402(2)	2.3(2)	0.8(1)	2.00	2.4(2)	180	2.95
0.10	5.8426(2)	2.4(2)	0.6(1)	2.00	2.5(2)	181	2.75
0.15	5.8462(5)	2.1(2)	0.7(1)	1.89	2.2(2)	168	3.07
0.20	5.8487(5)	2.2(2)		2.02	2.2(2)	161	2.92
1	5.8054(4)		1.1(1)		1.1(1)	−130	2.15

main crystallographic directions up to 9.5 T. The ordered ferromagnetic components of magnetic moments are strongly reduced if compared to μ_{eff}, and slightly decrease with increasing x. The hysteresis loops become broader with increasing Se content.

For $x=0.15$ and $H\simeq 5$ T we find a plateau in the hysteresis loop, which could indicate the presence of an intermediate phase. In addition, for $x\leqslant 0.15$, the easy axis changes with decreasing T from $\langle 111\rangle$ to $\langle 110\rangle$, indicating a transition to a different magnetic structure. For $x=0.05$ and 0.10 a deviation from normal ferromagnetic behavior is observed already below 150 K and for $x=0.15$ a transition is clearly observed around 75 K (see Fig. 4). This transition does not depend critically on applied field. The strong reduction of the net magnetization together with the variation of easy axis clearly indicate a complex ferrimagnetic ordering. At $x=0.20$ a different behavior is found for $H\geqslant 0.5$ T. There is no trace of the transition to the complex mixed structure. The sample has a first-order transition to a FM phase, with easy $\langle 111\rangle$ direction, at about 150 K.

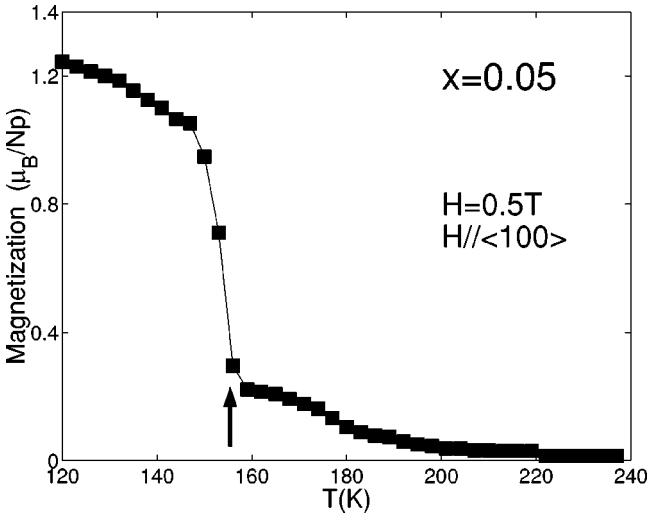

FIG. 3. Magnetization measurements in low field for $x=0.05$ clearly display the existence of two magnetic phases with a first-order transition between the two.

V. NEUTRON RESULTS

A. $x=0.05$

Measurements on this sample have been performed in zero magnetic field. In Fig. 5 we reproduce the evolution of the magnetic intensities given in Ref. 18. Above $T_N=175$ K only nuclear reflections allowed by the fcc symmetry are present. Below T_N extra intensities develop at the family of equivalent lattice position $\{k\,2\,0\}$ corresponding to a propagation vector $\vec{k}\approx[0.14(2)\,0\,0]$ that decreases as T is lowered. The same integrated intensities are obtained in the three directions $[k,2,0]$, $[2,k,0]$, and $[2,0,k]$, as expected for an fcc structure with equivalent domain volumes. The absence of intensity in the first Brillouin zone indicates that $\vec{m}$ is parallel to $\vec{k}$, where $\vec{m}$ is the Fourier component propagating along the wave vector $\vec{k}$. The measured intensity is re-

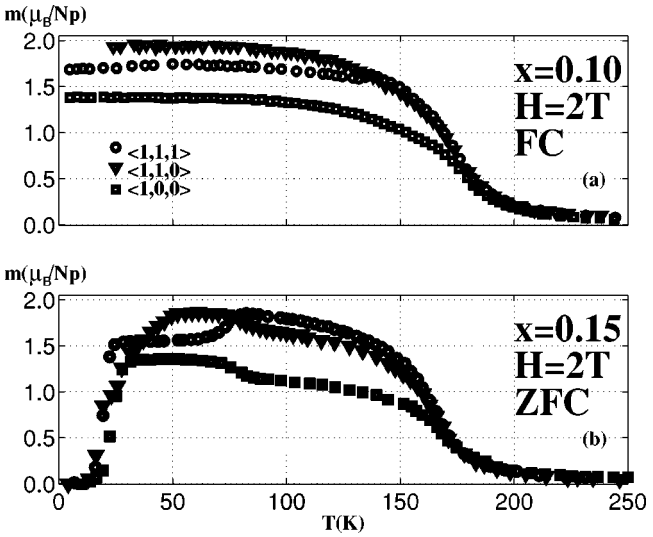

FIG. 4. Magnetization measurements on two samples ($x=0.10,0.15$) show the deviation from normal FM behavior. In (a) (field cooled, FC) at $T\simeq 150$ K the easy axes changes from $\langle 1\,1\,1\rangle$ to $\langle 1\,1\,0\rangle$. The moment below $T\simeq 100$ K stays almost constant. In (b) (zero field cooled, ZFC) the initial absence of a signal in the low-temperature low-field ($\vec{H}=2$ T) experiment is due to domain effects. By $T\simeq 50$ K a single domain is produced, the magnetization is independent of temperature, and the easy axis is $\langle 1\,1\,0\rangle$. This changes abruptly at $T=75$ K, where the easy axis becomes $\langle 1\,1\,1\rangle$.

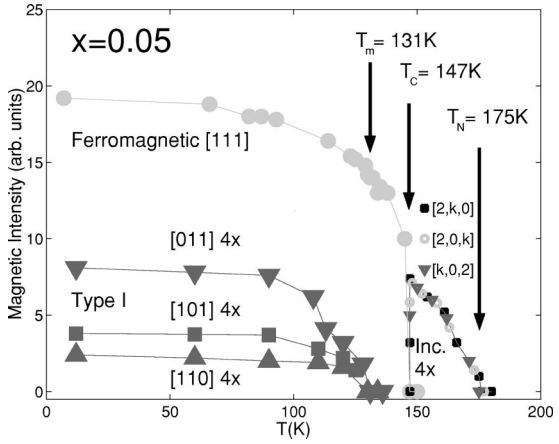

FIG. 5. Magnetic intensity measured by neutron diffraction on $NpAs_{1-x}Se_x$ (taken from Ref. 18). AF and incommensurate components are multiplied by 4. The arrows mark the temperatures of transition.

lated to an amplitude modulated collinear sinusoidal wave with $\vec{k}$ and $\vec{m}_{\vec{k}}$ parallel to the cubic axes. At $T \simeq 148$ K the amplitude of the Fourier component is $\simeq 1.7\mu_B$. On a further decrease of T the magnetic order changes. At $T_C = 147$ K the incommensurate intensity disappears and an extra magnetic contribution appears on the nuclear reflections. This signifies a first-order transition to FM. Due to the FM domains the moment direction cannot be determined by neutron diffraction but the magnetization data show that the easy direction is $\langle 1\,1\,1\rangle$. Decreasing T further, at $T_m = 131$ K (m=mixed) a magnetic contribution develops at $(0\,1\,1)$ and equivalent lattice positions, corresponding to the AF wave vector $\vec{k}=\langle 1\,0\,0\rangle$. The AF component is of type I. The three magnetic domains are not completely equivalent suggesting a $1\vec{k}$ rather than $3\vec{k}$ configuration, although this needs to be verified by applying a magnetic field.

B. $x = 0.10$

For this sample the evolution of magnetic intensities vs T in zero field is shown in Fig. 6. At $T_N \simeq 175$ K we measure a magnetic intensity in the lattice direction $[1\,1\,1-k]$ which

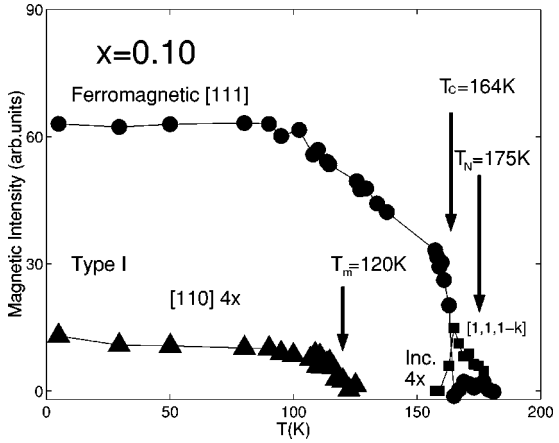

FIG. 6. Magnetic intensities measured by neutron diffraction. AF and incommensurate components are multiplied by 4. The arrows mark the temperatures of transition.

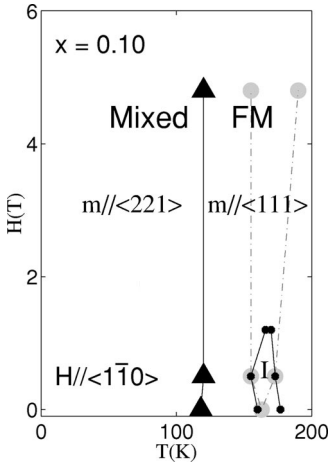

FIG. 7. Phase diagram for $x = 0.10$. Up to 4.8 T an AF component (triangles) is still present, whereas the incommensurate phase closes at about 1.2 T (small circles). In an external field the Curie temperature T_C is not well defined because of the high Np susceptibility that masks the real transition from PM to FM (dashed lines). At higher T circles mark the starting point of magnetic intensity on $[1\,1\,1]$ reflection and at the lower T the point at one-half of the height of the extra intensity. The maximum applied field of 4.8 T sets a lower limit to the anisotropy energy.

shows the existence of an incommensurate collinear phase with propagation vector $\langle 0\,0\,k\rangle$ where $\vec{k}$ decreases linearly with T from $k=0.17$ at ~ 175 K to $k=0.14$ at ~ 162 K. At ~ 164 K a first-order transition occurs to a FM phase ($k=0$) and magnetic moments are, as measured by magnetization, along the $\langle 1\,1\,1\rangle$ direction reaching $\simeq 2\mu_B$ at $T = 120$ K. This phase is not stable at low T. Around $T_m \simeq 120$ K a new peak develops at (110) and equivalent lattice positions, corresponding to an antiferromagnetic component ($k=1$) of type I, as in the $x=0.05$ sample.

The application of an external magnetic field along $[1\bar{1}0]$ allows us to determine the type of magnetic ordering. The external perturbation lifts the degeneracy between the three directions $[0\,0\,1]$, $[1\,0\,0]$, and $[0\,1\,0]$. In the case of a $1\vec{k}$ ordering only the domain with $\vec{k}$ (and $\vec{m}_{\vec{k}} \perp \vec{H}$) will survive, for a $3\vec{k}$ structure no change is expected in the AF intensity, whereas for a $2\vec{k}$ a more complex redistribution of intensity is expected. In our case, with $\vec{H}//[1\,\bar{1}\,0]$, only the peak at $(1\,1\,0)$ position survives and its intensity is about three times the zero-field intensity.

The phase diagram H-T for this sample is reported in Fig. 7. The incommensurate phase closes at about 1.2 T. The shift of FM phase to higher T is an effect of the high Np ion susceptibility. Up to 4.8 T the AF component does not change, and this is consistent with hysteresis loop that up to 10 T does not show any variation.

C. $x = 0.15$

At this concentration all the phases found at lower x are present. The main difference is that T_N and T_C now approach each other and there is little of the incommensurate phase. The AF component develops at $T_m \simeq 80$ K and, as in the other samples, this mixed phase is stable down to low T. An

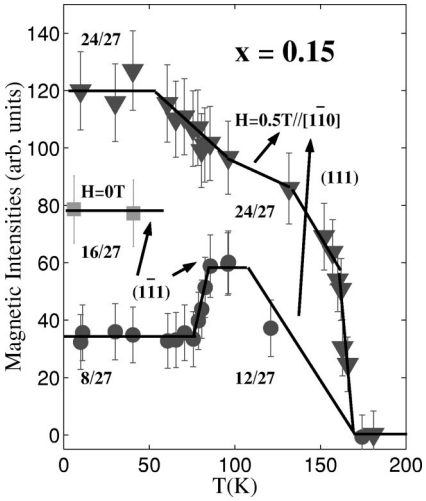

FIG. 8. Magnetic integrated intensities vs T measured on (111) peak (triangles) and ($\bar{1}11$) peak (circles). Sample is field cooled in a 0.5-T field. Data at low temperature in zero field for peak ($1\bar{1}\bar{1}$) are reported as squares. The effect of moment rotation due to the AF components is evident. Reported numbers are coefficients that originate from geometrical dependence of magnetic interactions (see text).

aspect that is very clear in this experiment is the rotation of the FM component of the magnetic moment. In fact the presence of AF ordering along the direction $[001]\perp\vec{H}$ in the mixed phase obliges the ferromagnetic component to be in the [110] direction. So the mixed phase occurring implies the FM moment rotation. This effect is easily verified by monitoring two nuclear reflections (Fig. 8). The measured magnetic intensities are $\propto\vec{m}_{FM}^2\langle\sin^2\alpha\rangle$ where $\vec{m}$ is the magnetic moment, $\langle\ \rangle$ is the average over $\hat{m}$ and α the angle between $\hat{m}$ and the diffraction vector $\hat{Q}$.

In zero field the intensities of the eight degenerate reflections {111} are equivalent, because moments in the crystal are equally distributed along these axes. As a consequence $\langle\sin^2\alpha\rangle=2/3$. Applying a field $\vec{H}||[1\bar{1}0]$ lifts the degeneracy. For $80\leqslant T\leqslant 170$ K (purely FM sample) $\vec{m}=\vec{m}_{FM}$ and moments are equally distributed along only two directions: $[1\bar{1}1]$ and $[\bar{1}\bar{1}1]$, which are closest to $\vec{H}$. If we consider the in-plane scattering (111) reflection $\langle\sin^2\alpha\rangle=24/27$, whereas the ($1\bar{1}1$) reflection that is $\simeq 30°$ out of the scattering plane gives $\langle\sin^2\alpha\rangle=12/27$. For $5\leqslant T<80$ K (mixed phase) $\vec{m}^2=\vec{m}_{FM}^2+\vec{m}_{AF}^2$, and on the nuclear reflections we measure only the FM component that is directed along $[1\bar{1}0]$, whereas the total moment is directed along an axis between $[1\bar{1}0]$ and $[1\bar{1}1]$. This gives for (111) reflection in applied field a $\langle\sin^2\alpha\rangle=1$, whereas for ($1\bar{1}\bar{1}$) $\langle\sin^2\alpha\rangle=1/3$. In order to compare directly with high-temperature FM phase we have to consider that $m_{FM}\simeq m_T\cdot 8/9$ and this causes a further reduction of the measured intensities.

D. $x=0.20$

A neutron experiment on the $x=0.20$ showed that it is FM at $T_C\sim 150$ K with probably a first-order phase transition to paramagnetism. No evidence for any AF component was found at $\vec{H}=0$.

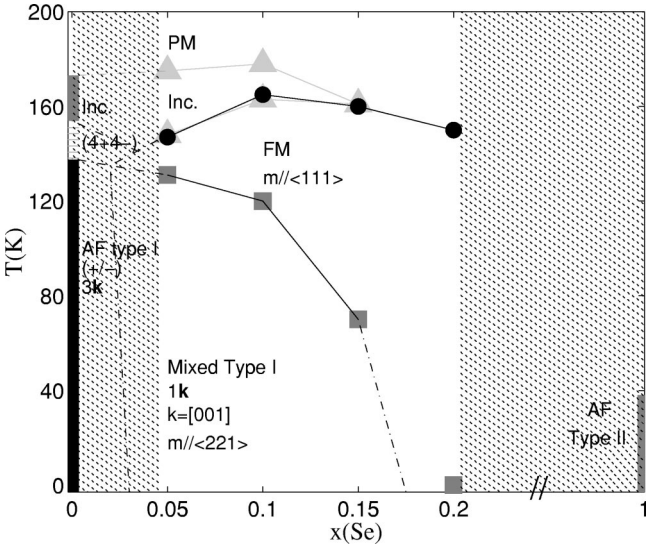

FIG. 9. Magnetic phase of $NpAs_{1-x}Se_x$ at zero field. Shaded regions are not yet explored. Magnetic behavior of pure NpAs ($x=0$) as well as pure NpSe ($x=1$) are reported. $x=0.05$ is enough to destroy completely the magnetic ordering found in pure NpAs. Various transitions are expected in the region $0.0<x<0.05$. The dashed lines indicate possible evolutions of the magnetic phases, presenting a multiphase point. The moment direction in NpSe is unknown.

VI. DISCUSSION

The phase diagram of $NpAs_{1-x}Se_x$ is reported in Fig. 9 and shows the evolution of the magnetic properties in zero field and increasing Se content. With increasing x the range of the incommensurate phase rapidly decreases, the mixed phase tends to lower T_m, whereas $T_C(x)$ increases slightly and then stays almost constant. The details of the transition between $x=0$ and $x=0.05$ are not yet investigated; a study of this region could reveal the existence of a multiphase point.

The magnetic moments arrangement at low T are similar for all low Se concentrations, and are shown in Fig. 10. The

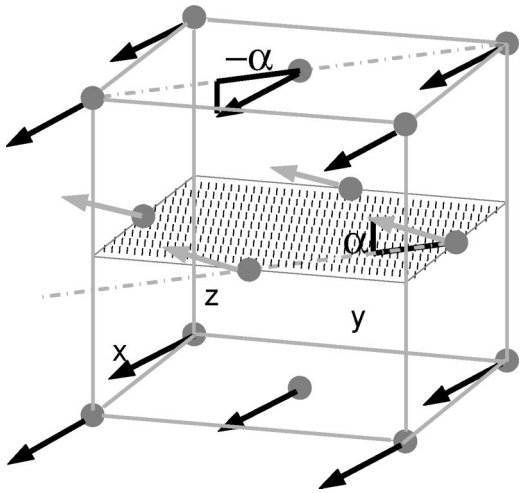

FIG. 10. Magnetic moment arrangement at low T in $NpAs_{1-x}Se_x$ with $0.05\leqslant x\leqslant 0.15$. In the domain shown the FM component is along [110] and the AF component along [001]. The angle α is $\simeq 18°$.

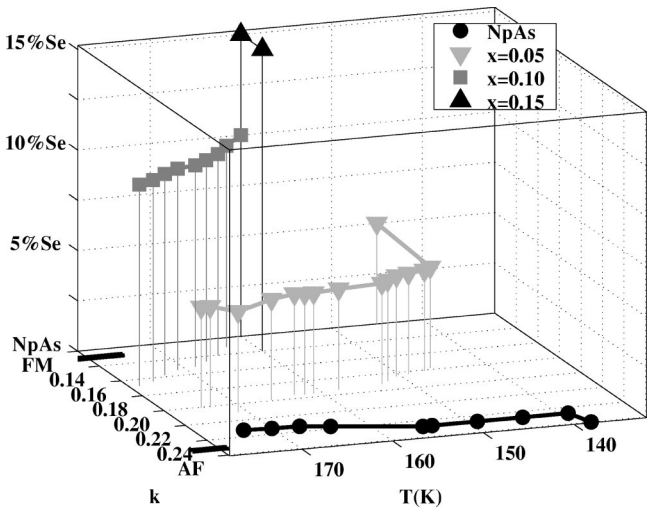

FIG. 11. Variation of the position of the center of the incommensurate contribution vs the T and the Se concentration.

magnetic moments lie in the plane defined by $\langle 1\,1\,1\rangle$ and $\langle 1\,1\,0\rangle$ and the angle with $\langle 1\,1\,0\rangle$ direction is about 18°. Previously, the only system studied in such a transuranium solid solution was NpSb-NpTe.[7] There are some similar features, but also some differences between the $NpSb_{1-x}Te_x$ and $NpAs_{1-x}Se_x$ systems. In both cases ferromagnetism appears at relatively low x, 0.10 in the NpSb-NpTe, and $x=0.20$ in the NpAs-NpSe compounds. The most notable similarity is that the *two* component magnetic structure (with both an AF and a FM component) was first identified in the $NpSb_{1-x}Te_x$ with $x=0.05$. A magnetic field was not applied to the sample in the neutron experiments reported, so that the information is not as complete as in our present study, but the underlying interactions are clearly similar. On the other hand, the initial ordering temperature (from the paramagnetic state) drops rapidly with x in the NpSb-NpTe system, whereas, as shown in Fig. 9, this is not the case in the system reported here.

Our experiments have opened a number of new perspectives on the study of solid solutions of transuranium compounds. The principal observations are as follows:

(i) The low-temperature type-I $3\vec{k}$ structure of NpAs is unstable. With a small change of the conduction-electron concentration, i.e., $x=0.05$, it disappears and the $1\vec{k}$ behavior that is found at high temperature even in NpAs returns as the ''stable magnetic phase.'' The $3\vec{k}$ magnetic structure in USb has been treated theoretically recently;[19] it would be interesting to extend these calculations to NpAs and consider the effects of a changing conduction-electron concentration on its $3\vec{k}$ ground state. With the resolution of D15 we are unable to determine the lattice symmetry of the $x=0.05$ sample. X-ray experiments are planned on this sample at low temperature.

(ii) A tendency to develop ferromagnetism with increasing x is found, and by $x=0.20$ the sample is ferromagnetic. A signature of this tendency is present also in the incommensurate phase (Fig. 11). The center of the incommensurate peaks shifts with increasing x and decreasing T toward the FM wave vector. This is similar to that found in the analogous UX-UY solid solution.[20] The fact that it is also found[21] in the doping of UX by tetravalent Th shows that the effect is mainly related to the conduction-electron concentration. However, it remains to extend the present studies to higher x as, unlike the case of doping UX with UY in which UY is ferromagnetic, in this case NpY is *antiferromagnetic*. It is clear that our experiments have not addressed this important question.

(iii) An unusual intermediate state is found between the tendency to have the Fourier components of the magnetization along $\langle 0\,0\,1\rangle$ in the AF state and $\langle 111\rangle$ in the FM state. Unlike in UX-UY solid solutions, in which the change between these two states is abrupt, in the case of $NpAs_{1-x}Se_x$ we find an intermediate state in the region $0.05\leqslant x\leqslant 0.15$ in which the moments actually rotate as a function of temperature. This is shown most clearly in the magnetization curves of Fig. 4 in which $\langle 1\,1\,0\rangle$ becomes the easy axis. This situation is observed directly in the neutron experiments in which the FM component rotates at T_m from the $\langle 111\rangle$ to $\langle 110\rangle$, and, simultaneously, an AF component develops along the $\langle 0\,0\,1\rangle$ axis perpendicular to the FM component (see Fig. 8). The resulting magnetic structure is shown in Fig. 10. The final components of the moments are almost along a $\langle 221\rangle$ direction, so that the total moment also slightly rotates. Since the strong spin-orbit coupling in actinides favors magnetic moments along the high symmetry directions[22] this situation is rather unusual, and suggests that a balance between the single-ion anisotropy and the magnetic exchange determines the magnetic structures. However, despite this compromise leading to a rather unusual easy axis, the anisotropy in the system far exceeds any normal laboratory magnetic field, as shown by the experiment we have performed at 5 T. The latter is not sufficient to change the direction of the magnetization. Anisotropies of this magnitude are common in actinide systems, and are thought to arise from the hybridization between the actinide $5f$ and anion p electrons.[2] This unusual situation in the lightly doped NpAs compounds gives a further test for theories developed to understand these anisotropies.

(iv) We note that in these pseudobinary Np solid solutions the lattice parameter (Table II) does not follow the Vegard law vs x. In all the diluted samples the lattice parameter measured by x-ray diffraction[23] at room temperature are bigger than those of their parent compounds, coming closer to the lattice parameter of the PuAs, which is a ferromagnet.

Our experiments have completed the preliminary studies reported[18] for $x=0.05$ and revealed a rich behavior in the small doping limit of NpAs. However, still remaining is to explore the region of the phase diagram near $x=1$, when another transition from FM to AF, but this time of type II, must occur.

ACKNOWLEDGMENTS

A. Bombardi acknowledges the European Commission for support given in the frame of the program ''Training and Mobility of the Researchers.'' The high-purity Np metal required for the fabrication of the compounds studied here was made available through a loan agreement between Lawrence Livermore National Laboratory and Institute for Transuranium Elements, in the frame of a collaboration involving LLNL, Los Alamos National Laboratory, and the U.S. Department of Energy.

[1] O. Vogt and K. Mattenberger, in *Handbook on the Physics and Chemistry of the Rare Earths*, edited by K. A. Gschneidner, Jr., L. Eyring, G. H. Lander, and G. R. Choppin (North-Holland, Amsterdam, 1993), Vol. 17, Chap. 114.

[2] B. R. Cooper, R. Siemann, D. Yang, P. Thayamballi, and A. Banerjea, in *Handbook on the Physics and Chemistry of the Actinides*, edited by A. Freeman and G. H. Lander (North-Holland, Amsterdam, 1985), Vol. 2, Chap. 6.

[3] P. Wachter, in *Handbook on the Physics and Chemistry of the Rare Earths*, edited by K. A. Gschneidner, Jr., L. Eyring, G. H. Lander, and G. R. Choppin (North-Holland, Amsterdam, 1994), Vol. 19, p. 177.

[4] P. M. Oppeneer, T. Kraft, and M. S. S. Brooks, Phys. Rev. B **61**, 12 825 (2000).

[5] J. Rossat-Mignod, G. H. Lander, and P. Burlet, in *Handbook on the Physics and Chemistry of the Actinides*, edited by A. Freeman and G. H. Lander (North-Holland, Amsterdam, 1984), Vol. 1, Chap. 6.

[6] G. H. Lander, in *Handbook on the Physics and Chemistry of the Rare Earths* (Ref. 1), Vol. 17, Chap. 117.

[7] K. Mattenberger, O. Vogt, J. Rebizant, J. C. Spirlet, P. Burlet, E. Pleska, and J. Rossat-Mignod, Physica B **163**, 488 (1990).

[8] P. Burlet, S. Quezel, M. Kuznietz, D. Bonnisseau, J. Rossat-Mignod, J. C. Spirlet, J. Rebizant, and O. Vogt, J. Less-Common Met. **121**, 325 (1986).

[9] P. Burlet, D. Bonnisseau, S. Quezel, J. Rossat-Mignod, J. C. Spirlet, J. Rebizant, and O. Vogt, J. Magn. Magn. Mater. **63-64**, 151 (1987).

[10] D. L. Jones, W. G. Stirling, G. H. Lander, J. Rebizant, J. C. Spirlet, M. Alba, and O. Vogt, J. Phys.: Condens. Matter **3**, 3551 (1991).

[11] S. Langridge, W. G. Stirling, G. H. Lander, and J. Rebizant, Phys. Rev. B **49**, 12 010 (1994).

[12] A. T. Aldred, B. D. Dunlap, A. R. Harvey, D. J. Lam, G. H. Lander, and M. H. Mueller, Phys. Rev. B **9**, 3766 (1974).

[13] U. Potzel, J. Moser, W. Potzel, S. Zwirner, W. Schiessl, F. J. Litterst, G. M. Kalvius, J. Gal, S. Fredo, S. Tapuchi, and J. C. Spirlet, Hyperfine Interact. **47**, 399 (1989).

[14] A. Blaise, M. N. Bouillet, F. Bourdarot, P. Burlet, J. Rebizant, J. Rossat-Mignod, J. P. Sanchez, J. C. Spirlet, and O. Vogt, J. Magn. Magn. Mater. **104-107**, 33 (1992).

[15] J. C. Spirlet and O. Vogt, in *Handbook on the Physics and Chemistry of the Actinides* (Ref. 5), Vol. 1, p. 79.

[16] W. Potzel, G. M. Kalvius, and J. Gal, in *Handbook on the Physics and Chemistry of the Rare Earths* (Ref. 1), Vol. 17, Chap. 116.

[17] J. P. Sanchez, K. Tomala, J. Rebizant, J. C. Spirlet, and O. Vogt, Hyperfine Interact. **54**, 701 (1990).

[18] K. Mattenberger, O. Vogt, J. Rebizant, J. C. Spirlet, F. Bourdarot, P. Burlet, J. Rossat-Mignod, M. N. Bouillet, A. Blaise, and J. P. Sanchez, J. Magn. Magn. Mater. **104-107**, 43 (1992).

[19] H. Yamagami, Phys. Rev. B **61**, 6246 (2000).

[20] M. Kuznietz, P. Burlet, J. Rossat-Mignod, and O. Vogt, J. Less-Common Met. **121**, 217 (1986); J. Magn. Magn. Mater. **69**, 12 (1987).

[21] J. A. Paixão, G. H. Lander, C. C. Tang, W. G. Stirling, A. Blaise, P. Burlet, P. J. Brown, and O. Vogt, Phys. Rev. B **47**, 8634 (1993).

[22] L. M. Sandratskii, Adv. Phys. **47**, 91 (1998).

[23] F. Wastin, J. C. Spirlet, and J. Rebizant, J. Alloys Compd. **219**, 232 (1995).